

## Thermal stability of diazodinitrophenol

M. Kaiser \*, U. Ticmanis

*Bundesinstitut für chemisch-technische Untersuchungen (BICT), Großes Cent,  
53913 Swisttal-Heimerzheim, Germany*

Received 28 January 1994; accepted 5 July 1994

---

### Abstract

The stability of diazodinitrophenol in the solid phase has been investigated by four different thermoanalytical methods and by  $^1\text{H}$  NMR spectroscopy. The results show that the substance is stable for long periods at temperatures below  $60^\circ\text{C}$ . A kinetic relation has been developed, which permits the calculation of the degree of reaction at given storage temperatures and times.

*Keywords:* Diazodinitrophenol; DSC; IDSC; Kinetics; Stability; VITG

---

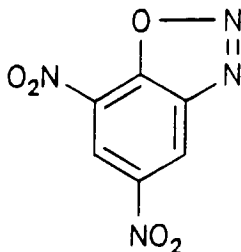
### 1. Introduction

Although diazodinitrophenol (DDNP) has been known since 1858 [1] this primary explosive has not been used in German ammunition. The health risk to staff in enclosed rifle ranges posed by heavy metal reaction products led to the development of the SINTOX compositions [2] which contain a high quantity of DDNP in addition to tetracene, zinc peroxide and titanium. It was not clear whether the new compositions guaranteed the lifetime demanded for long period storage for the following reasons:

(1) The decomposition temperature  $T_z$  of DDNP (the lowest temperature at which an exothermic reaction can be detected under standardized conditions (heating rate  $5\text{ K min}^{-1}$ ; sample mass, 1–5 mg)) is markedly below that of tetracene

---

\* Corresponding author.



Formula 1. Diazodinitrophenol (DDNP).

Table 1  
Decomposition temperatures of some primary explosives

| Primary explosive | $T_d/^\circ\text{C}$ |
|-------------------|----------------------|
| DDNP              | 142                  |
| Tetracene         | 146                  |
| Lead styphnate    | 252                  |

and considerably below those of other primary explosives, e.g. lead styphnate as can be seen from Table 1. The temperatures to which the substances may be subjected during long term storage are, of course, far below the dynamic decomposition temperatures.

(2) In the literature the thermal decomposition of DDNP is characterized by an activation energy between 67 and 178 kJ mol<sup>-1</sup> and various frequency factors [3–5]. Because the description of the process requires a complete kinetic relation (especially if the reaction is autocatalytic) a reliable extrapolation of the long term behaviour at room temperature is not possible with the existing data.

In view of this extrapolation problem the kinetic relations must be determined as accurately as possible. The probability of errors is reduced if different methods give closely related results. For that reason a bundle of methods has been employed.

## 2. Apparatus and measurement

Dynamic differential scanning calorimetry (DSC) and isothermal differential scanning calorimetry (IDSC) investigations were carried out on a Mettler TA 3000 thermoanalysis system. For these measurements, closed aluminium pans with a vent in the lid in flowing nitrogen atmosphere were used. DSC investigations were carried out with samples of about 1.4 mg sample size and heating rates between 0.1 and 10°C min<sup>-1</sup>, whereas in the IDSC measurements samples of about 4 mg were heated at 120, 130 and 140°C.

Isothermal thermogravimetric measurements (ITG) were made in an oven at  $104 \pm 0.5^\circ\text{C}$ . Aluminium vessels of 0.1 ml volume loosely closed with a cap and samples of about 25 mg were used. The vessel was weighed on a microbalance after cooling to room temperature. The results were corrected to equal buoyancy by weighing of an empty vessel.

Varying isothermal thermogravimetry (VITG) was carried out with a NETSCH simultaneous thermal analyser STA 429. The same closed aluminium pans but containing about 100 mg DDNP were heated in air flowing at a rate of  $50 \text{ ml min}^{-1}$ . The first sample was measured at 90 and  $110^\circ\text{C}$  in 12 cycles up to a mass loss of 28%. The second sample was investigated at 100 and  $120^\circ\text{C}$  in seven cycles to the same mass loss.

NMR spectroscopic investigations were carried out with a BRUKER CXP-100 NMR instrument at 90 MHz frequency. The substances from the ITG experiments with different mass losses were dissolved in 0.9 ml deuterated dimethylsulphoxide and the  $^1\text{H}$  NMR spectra were recorded.

### 3. Determination of the activation energy

The activation energy was determined by different methods. The aim of this procedure is to test whether Eq. (1) is able to describe the process with sufficient accuracy or whether equations with more than one activation energy must be considered.

$$d\alpha/dt = f(\alpha)A e^{-E/RT} \quad (1)$$

where  $\alpha$  is the degree of reaction,  $t$  is the reaction time,  $d\alpha/dt$  is the reaction rate,  $T$  is the temperature of reaction,  $A$  is the pre-exponential factor or frequency factor,  $E$  is the activation energy,  $f(\alpha)$  is the reaction model (RM), and  $R$  is the gas constant.

Knowledge of the reaction model (RM) is not necessary because only points with equal degrees of reaction (iso- $\alpha$ -points) are evaluated. At these points the RM and all functions derived from it have the same value and are thus eliminated. If a constant activation energy is determined, the validity of Eq. (1) is proved. Results from DSC, IDSC and VITG have been examined.

#### 3.1. Activation energy from DSC measurements

The measurements at heating rates of  $0.1$  to  $1 \text{ K min}^{-1}$  are shown in Fig. 1. It was shown by model calculations for different RM in Eq. (1) that the degree of reaction at the maximum reaction rate  $\alpha_m$  is nearly constant, even if the heating rate is changed by a factor of 100 [6]. Therefore the peak maxima are to a good approximation iso- $\alpha$ -points. Two of the three procedures for testing Eq. (1) are therefore based on peak points.

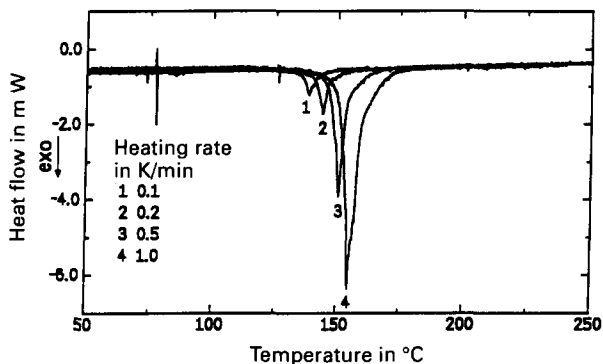


Fig. 1. Results of the dynamic DSC measurements.

### 3.1.1. From peak temperatures ( $T_m$ ) and heating rates

The generalized derivation of Kissinger [7] leads to

$$\ln(H/T_m^2) = \ln(RA/EC) - E/RT_m \quad (2)$$

where  $H$  is the heating rate, with  $C = -1/f'(\alpha_m)$ . The evaluation according to this equation (Fig. 2) shows a change of kinetics at 155°C which is due to the melting of the DDNP [5,8]. The kinetics in the higher temperature region are not relevant for the problem considered here. The decomposition of the solid DDNP in the lower region is obviously approximated well by Eq. (1). The activation energy is calculated as  $E = 177.3 \text{ kJ mol}^{-1}$ .

### 3.1.2. From peak temperatures and peak heights

If the peak heights are normalized to equal amounts of sample Eq. (1) can be written as

$$\ln(P/M) = \ln[f'(\alpha_m)A'] - E/RT_m \quad (3)$$

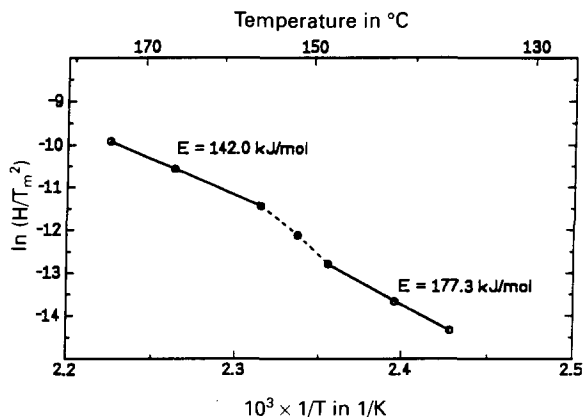


Fig. 2. Kissinger evaluation of activation energy.

where  $P$  is the peak heights,  $A'$  is a constant proportional to the frequency factor, and  $M$  is the sample mass.

This evaluation of the measurements with heating rates of  $H = 0.1, 0.2$  and  $0.5$   $\text{K min}^{-1}$ , corresponding to the solid phase, also confirm the proposed main equation (Fig. 3). An activation energy  $E = 181.8$   $\text{kJ mol}^{-1}$  was determined.

### 3.1.3. From reaction rates using the Friedman [9] analysis

Integration of the peak areas using the measurements with the heating rates of  $0.1, 0.2, 0.5$  and  $1$   $\text{K min}^{-1}$  gives the heat of reaction  $\Delta H$  as  $1851 \pm 31$   $\text{J g}^{-1}$ . After transformation of the data to the  $\alpha$  form using  $\alpha = dH/\Delta H$  and  $d\alpha/dt = (dQ/dt)/\Delta H$  (where  $dH$  is the first part of the peak area at a given reaction temperature and  $dQ/dt$  is the heat flux) the activation energy at different iso- $\alpha$ -points can be determined from the logarithmic form of Eq. (1). Points at temperatures greater than  $154^\circ\text{C}$ , corresponding to the molten phase, were neglected. The result is shown in Fig. 4. Up to  $\alpha = 0.7$  the activation energy can be regarded as constant. The average value in the region from  $\alpha = 0.1$  to  $0.7$  is  $E = 181.7 \pm 7.9$   $\text{kJ mol}^{-1}$ .

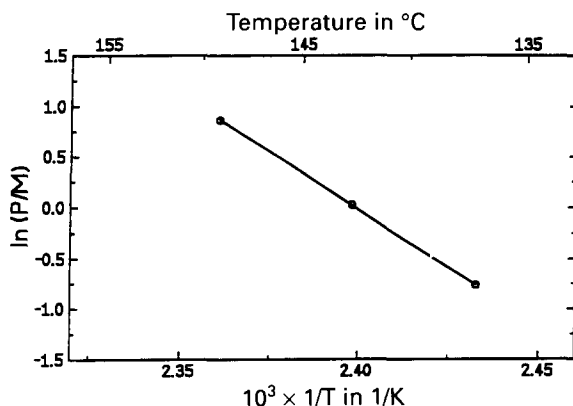


Fig. 3. Arrhenius plot from peak temperatures and heights.

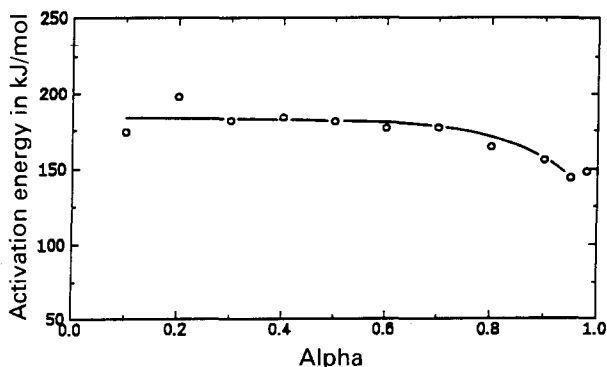


Fig. 4. Activation energy by Friedman analysis.

### 3.2. Activation energy from IDSC measurements

Dynamic calorimeters are generally not suitable for quantitative isothermal investigations. This is shown by our measurements in Fig. 5. However, the autocatalytic reaction type is clearly demonstrated and the reaction times  $t_m$  ( $t_1$ ,  $t_2$ ,  $t_3$ ) up to the maxima (M1, M2, M3) can be determined relatively precisely. Because the peaks are iso- $\alpha$ -points, this is again sufficient for testing Eq. (1). The integration of Eq. (1) leads to

$$\ln t_m = \ln C + E/RT \quad (4)$$

where  $C = \ln[1/A \int_0^m d\alpha/f(\alpha)]$ . The measured reaction times correspond to this equation (Fig. 6). The activation energy  $E$  was  $180.1 \text{ kJ mol}^{-1}$  and  $C$  was calculated to be  $1.049 \times 10^{-21}$ .

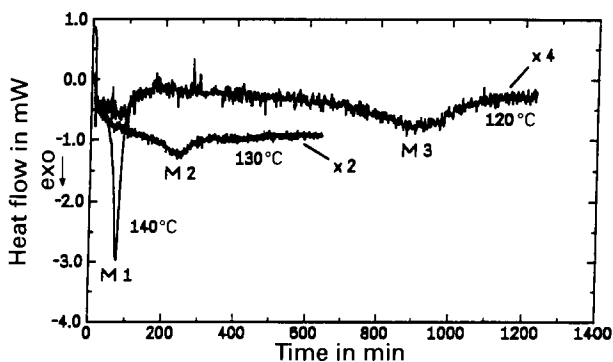


Fig. 5. Results of isothermal DSC measurements.

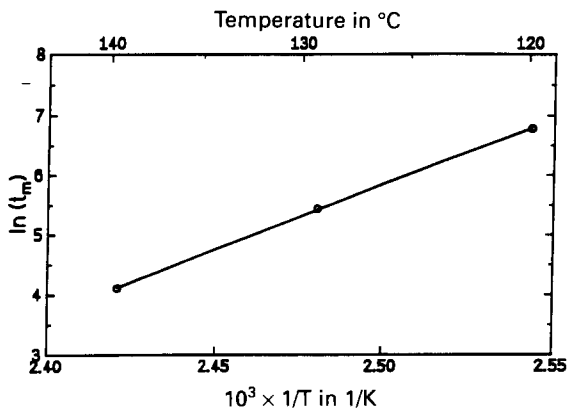


Fig. 6. Arrhenius plot derived from reaction times (in minutes) and temperatures.

Table 2  
Activation energies obtained by different methods

| Method                                | $E/\text{kJ mol}^{-1}$ |
|---------------------------------------|------------------------|
| DSC (peak temperatures/heating rates) | 177.3                  |
| (peak temperatures/peak heights)      | 181.8                  |
| (Friedman analysis)                   | 181.7                  |
| IDSC                                  | 180.1                  |
| VITG                                  | 178                    |

### 3.3. VITG measurements

With the help of the differentiated mass loss ( $G$ )–time curve, Eq. (1) was checked in the form of

$$\ln(dG/dt) = \ln[f(G)A''] - E/RT \quad (5)$$

where  $A''$  is a factor which is proportional to the frequency factor, at points of equal mass loss (iso- $G$ -points) between Sample 1 (90/110°C) and Sample 2 (100/120°C). The evaluation showed an activation energy  $E$  of  $178 \pm 10 \text{ kJ mol}^{-1}$  in the region  $G = 0.4\%$  to  $16\%$ . At higher reaction volumes ( $G > 25\%$ ), which are not interesting in this case, a slow second reaction with an activation energy  $E$  of  $145 \text{ kJ mol}^{-1}$  is observed.

### 3.4. Summary of the activation energy tests

The results of the three methods (Table 2) show that the thermal decomposition of DDNP can be described well by Eq. (1). The calculated values of the activation energies scatter only slightly. Because of the evaluation of a greater reaction range and at lower temperatures the VITG value is regarded as the most reliable result.

## 4. Determination of the reaction model

After proving the general equation and determination of the activation energy a suitable reaction model  $f(\alpha)$  has to be generated, which describes the relationship between rate and degree of reaction. The IDSC measurements (see Fig. 5) show the autocatalytic type of the reaction. This means that  $f(\alpha)$  is a function with a maximum. By examining the first parts of the VITG measurements it was found that  $f(0) \neq 0$ . Both properties indicate an  $n$ th order RM with autocatalysis. Therefore the equation

$$f(\alpha) = (1 - \alpha)^n [1 + (a - 1)\alpha] \quad (6)$$

where  $a$  is a catalysis constant, should solve the problem.

In order to estimate the RM constants  $n$  and  $a$ , some considerations of the regression forms and criteria should be carried out. Using the mass loss as a measure of the degree of reaction and  $G_e$  as the final value for the total reaction, Eq. (6) can be transformed to

$$f(G) = (1 - G/G_e)^n [1 + (a - 1)G/G_e] \quad (7)$$

Equation (1) in combination with Eq. (6) or Eq. (7) gives the complete equations for constant temperature

$$d\alpha/dt = (1 - \alpha)^n [1 + (a - 1)\alpha]k \quad (8)$$

and

$$dG/dt = (1 - G/G_e)^n [1 + (a - 1)G/G_e]k' \quad (9)$$

where  $k = A e^{-E/R^*T}$  and  $k' = kG_e$ .

Integration and transformation of Eqs. (8) and (9) gives

$$t = (1/k) \int_0^\alpha d\alpha / (1 - \alpha)^n [1 + (a - 1)\alpha] \quad (10)$$

and

$$t = (1/k') \int_0^G dG / (1 - G/G_e)^n [1 + (a - 1)G/G_e] \quad (11)$$

If  $n = 1$  the integrals can be solved, which results in

$$\alpha = (e^{akt} - 1) / (e^{akt} - 1 + a) \quad (12)$$

and

$$G = G_e (e^{akt} - 1) / (e^{akt} - 1 + a) \quad (13)$$

Generally explosives are no longer of use after a small fraction has decomposed. This demands a very sure knowledge of the first reaction range and means that short times (Eqs. (10) and (11)) or small  $\alpha$  values (Eqs. (12) and (13)) should be weighted more than in the normal (absolute) least squares fitting. Therefore we use the minimization of the relative error sum  $\sum f_{rel}^2$ . In a general equation of the form

$$y = f(x, z, \dots) \quad (14)$$

this sum is

$$\sum f_{rel}^2 = \sum [1 - f(x, z, \dots)/y]^2 \quad (15)$$

It should be noted that the equivalent  $y$  display is of logarithmic type. Therefore in normal display the higher values seem to have greater deviations.

#### 4.1. Model constants from NMR investigations

In contrast to integral thermoanalytical methods, it is possible in NMR spectroscopy to determinate the amount of the starting molecules and therefore the



degree of the primary reaction can be calculated. Figure 7 shows the  $^1\text{H}$  NMR spectra of the starting material and the reaction mixture after 9 days storage at  $104^\circ\text{C}$ . The signals at  $\delta = 8.87$  and  $\delta = 9.33$  are due to the aromatic protons of DDNP. The solvent signal appears at  $\delta = 2.49$  and that of the contained water at  $\delta = 3.8$ . The DDNP signals have become very small after storage. Some other signals appear at  $\delta = 7.78$  and  $\delta = 8.21$  and belong to an intermediate reaction product. The final product causes a broad signal between  $\delta = 7.8$  and  $\delta = 9.1$ . Integration of all protons in the spectrum and comparison with the starting substance demonstrates that the total amount of the protons remains in the solid phase.

One obtains the degree of reaction from

$$\alpha = 1 - \frac{\sum {}^1H_t}{\sum {}^1H_0} \quad (16)$$

where  $\sum {}^1H_t$  is the NMR peak area of DDNP after storage time  $t$  and  $\sum {}^1H_0$  is the NMR peak area of unreacted DDNP.

Optimization of the constants ( $k$ ,  $n$ ,  $a$ ) in Eq. (10) gave a best reaction order near unity. For this reason  $n = 1$  was accepted and the regression was repeated with Eq. (12) which results in  $a = 67.00$  and  $k = 0.01156 \text{ d}^{-1}$ . Figure 8 shows the good reproduction of the measured data points by the theoretical curve.

#### 4.2. Model constants from ITG measurements

Optimization of the constants  $k$ ,  $n$ ,  $a$  and  $G_e$  according to Eq. (11) leads once again to a reaction order close to unity. A second regression with Eq. (13), where

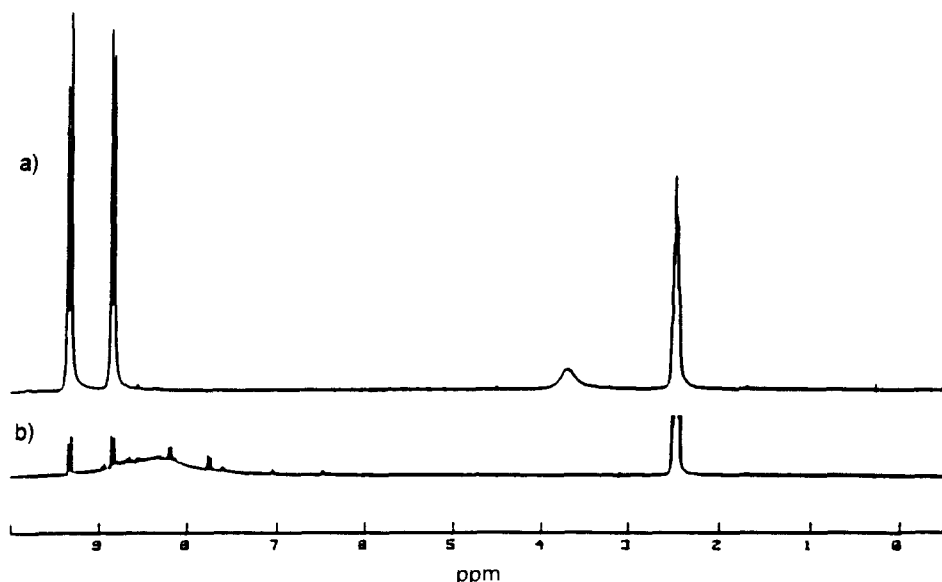


Fig. 7. Results of  $^1\text{H}$  NMR measurement of DDNP: (a) unreacted (b) stored at  $104^\circ\text{C}$  for 9 days.

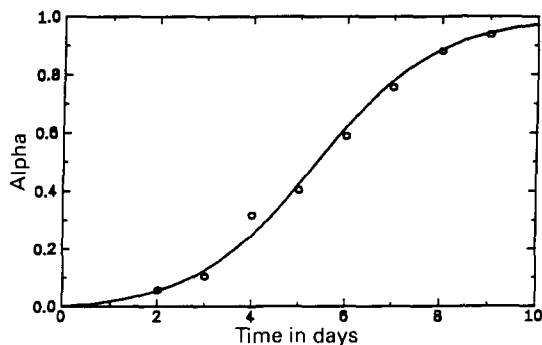


Fig. 8. Experimental NMR data fitted with reaction model which is first order with autocatalysis.

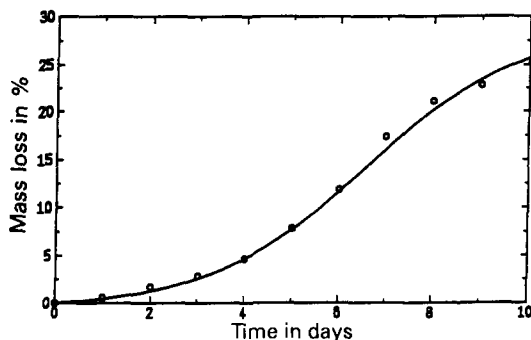


Fig. 9. Experimental ITG data fitted with a first order model with autocatalysis.

$n = 1$ , gave the following values:  $a = 51.06$ ,  $k = 0.01161 \text{ d}^{-1}$  and  $G_e = 29.19$ . In Fig. 9 the model curve shows a satisfactory fit to the experimental data covering almost the whole range of measurement. The secondary reaction is significant only at mass losses higher than 20% and therefore it can be neglected for our purposes.

The fittings show that the first order RM with autocatalysis is capable of describing the thermal decomposition of DDNP. NMR and ITG data lead to similar values for the model constant  $a$  and almost identical values of the velocity constant  $k$ . The last fact means that both methods describe as desired the first range of the reaction in a very similar way. Due to their selectivity the NMR data were chosen for stability calculations.

## 5. Kinetic equation from NMR and VITG

Solving Eq. (12) for time and substituting  $k$  with  $A e^{-E/RT}$  gives

$$t = \ln[a/(1/\alpha - 1) + 1]/aA e^{-E/RT} \quad (17)$$

The constants from NMR and VITG are  $a = 67.00$ ,  $A = 5.218 \times 10^{22} \text{ d}^{-1}$  and  $E = 178 \text{ kJ mol}^{-1}$ ; the abbreviated name of this equation is the “NMR/TG kinetic” equation.

## 6. Kinetic compatibility of the methods

Before Eq. (17) was used to extrapolate long term stability, a satisfactory reproduction of the IDSC and DSC results not involved in this equation has been examined. Similarly to the activation tests, neither method assumes a knowledge of the reaction model.

### 6.1. Comparison between NMR/TG and IDSC

The times required to reach the reaction maximum upon isothermal storage were calculated from both methods and compared. It can be seen from the data in Table 3 that both methods gave satisfactory corresponding reaction times even in the extrapolated range.

### 6.2. Comparison between NMR/TG and DSC

The times  $t_{\text{DSC}}$  to reach any specified degree of reaction at isothermal storage can also be calculated from the dynamic DSC data by

$$t_{\text{DSC}} = (1/H) \int_0^{T_{\text{DSC}}} e^{-E/RT} dT e^{E/RT_{\text{ISO}}} \quad (18)$$

where  $T_{\text{DSC}}$  is the DSC temperature at which the reference degree of reaction is reached,  $T_{\text{ISO}}$  is the isothermal storage temperature, and  $E$  is the activation energy from the Kissinger evaluation.

For comparison with NMR/TG we use the measured  $T_{\text{DSC}}$  temperatures of the dynamic maximum to calculate the isothermal times  $t_{\text{DSC}}$  from Eq. (18). As before

Table 3  
Times required to reach reaction maximum upon isothermal storage

| Temp./°C | $t_{\text{IDSC}}^a$ | $t_{\text{NMR/TG}}^b$ |                    |
|----------|---------------------|-----------------------|--------------------|
| 140      | 62,2 min            | 55 min                | Measured range     |
| 130      | 227 min             | 199 min               |                    |
| 120      | 890 min             | 769 min               |                    |
| 100      | 12 days             | 10 days               | Extrapolated range |
| 80       | 317 days            | 255 days              |                    |
| 60       | 34 years            | 27 years              |                    |

<sup>a</sup> Calculated from Eq. (4) with the constants from IDSC measurements.

<sup>b</sup> Calculated from Eq. (17) for the theoretical decomposition degree ( $\alpha = 0.492$ ) of the isothermal reaction maximum.

Table 4

Times required to reach reaction maximum upon isothermal storage

| Temp./°C | $t_{\text{DSC}}^{\text{a}}$ | $t_{\text{NMR/TG}}^{\text{b}}$ |                    |
|----------|-----------------------------|--------------------------------|--------------------|
| 140      | 65,1 min                    | 61 min                         | Measured range     |
| 130      | 234 min                     | 220 min                        |                    |
| 120      | 899 min                     | 847 min                        |                    |
| 100      | 11 days                     | 11 days                        |                    |
| 80       | 291 days                    | 281 days                       | Extrapolated range |
| 60       | 30 years                    | 29 years                       |                    |

<sup>a</sup> Calculated from Eq. (18). <sup>b</sup> Calculated from Eq. (17) for the theoretical dynamic maximum  $\alpha = 0.598$ .

the  $t_{\text{NMR/TG}}$  times were calculated from Eq. (17) but now they have been calculated for the theoretical dynamic maximum ( $\alpha = 0.598$ ). Again the agreement of both methods is satisfactory (Table 4). The calculated data differ little in the measured and extrapolated range.

### 6.3. Control of long term storage with NMR/TG

Spear and Maksacheff [10] determined the “half time” of the thermal decomposition of DDNP stored at 89°C to be 50 days. In satisfactory agreement, with  $\alpha = 0.5$ , Eq. (17) gives a value of 57 days.

### 6.4. Evaluation of NMR/TG kinetics

In comparison, all methods employed gave results which differ only slightly from NMR/TG kinetics. This is also true for extrapolations towards lower temperatures. Equation (17) is therefore considered to be a reliable basis for stability estimations of DDNP.

Table 5

Values of  $t_{0.02}$  calculated using Eq. (17)

| Storage temperature/°C | $t_{0.02}$ |
|------------------------|------------|
| 100                    | 2.0 days   |
| 90                     | 9.9 days   |
| 80                     | 52 days    |
| 70                     | 307 days   |
| 60                     | 5.5 years  |
| 50                     | 40 years   |

## 7. Calculation of the application time of DDNP

It is supposed that a reaction degree of  $\alpha = 0.02$  (0.6% mass loss) can be accepted for all uses of DDNP. The  $t_{0,02}$  times can therefore be considered as the minimum application times. These times have been calculated from Eq. (17) for different storage temperatures; results are shown in Table 5. It can be seen that DDNP is destroyed quickly at temperatures of more than 100°C. At moderate temperatures, however, it is stable for long periods.

## References

- [1] P. Griess, *Justus Liebigs Ann. Chem.*, 106 (1858) 123.
- [2] R. Hagel and K. Redecker, *Propellants Explos.*, 11 (1986) 184.
- [3] K. Yamamoto, *Explosifs*, 18 (1965) 14.
- [4] M.M. Jones and H.J. Jackson, *Explosivstoffe*, 9 (1959) 180.
- [5] D.J. Whelan and R.J. Spear, *Thermochim. Acta*, 80 (1984) 149.
- [6] U. Ticmanis, BICT-Rep. 330/7656/88, 29 July 1988, Bundesinstitut für chemisch technische Untersuchungen, Großes Cent, 53913 Swisttal-Heimerzheim, Germany.
- [7] H.E. Kissinger, *Anal. Chem.*, 29 (1957) 1702.
- [8] A.A. Duswalt, *Analytical Calorimetry*, Plenum Press, New York, 1968, p. 313.
- [9] H.L. Friedman, *J. Polym. Sci.*, C6 (1965) 183.
- [10] R.J. Spear and M. Maksacheff, *Thermochim. Acta*, 105 (1986) 287.